Insulator-to-Metal Phase Transition in a Few-Layered $MoSe_2$ Field Effect Transistor

Journal:	*Nanoscale*
Manuscript ID	NR-ART-09-2022-005019.R1
Article Type:	Paper
Date Submitted by the Author:	24-Dec-2022

Complete List of Authors:	Pradhan, Nihar; Jackson State University, Physics; National High Magnetic Field Laboratory, Condensed Mater Physics Garcia, Carlos; National High Magnetic Field Laboratory; Florida State University, Physics Chakrabarti, Bhaswar; Argonne National Laboratory, Center for Nanoscale Materials; University of Chicago, Institute for Molecular Engineering; Indian Institute of Technology Madras, Electrical Engineering Rosenmann, Daniel; Argonne National Laboratory, Divan, Ralu; Argonne National Laboratory, Center for Nanoscale Materials Sumant, Anirudha; Argonne National Laboratory, Centre for NanoMaterials Miller, Suzanne; Argonne National Laboratory, Center for Nanoscale Materials Hilton, David; Baylor University, Department of Physics Karaiskaj, Denis; University of South Florida, Department of Physics McGill, Stephen; National High Magnetic Field Laboratory,

Insulator-to-Metal Phase Transition in a Few-Layered $MoSe_2$ Field Effect Transistor

Nihar R. Pradhan[1,2,*], Carlos Garcia[2], Bhaswar Chakrabarti[3,4], Daniel Rosenmann[3], Ralu Divan[3], Anirudha V. Sumant[3], Suzanne Miller[3], David Hilton[5], Denis Karaiskaj[6], and Stephen A. McGill[2*]
[1]*Layered Materials and Device Physics Laboratory, Department of Chemistry, Physics and Atmospheric Science, Jackson State University, Jackson, MS 39217, USA*
[2]*National High Magnetic Field Laboratory, Tallahassee, FL 32310, USA*
[3]*Center for Nanoscale Materials, Argonne National Laboratory, 9700 S-Cass Avenue, Lemont, IL-60439, USA*
[4]*Department of Electrical Engineering, Indian Institute of Technology Madras, Chennai, Tamil Nadu- 600036, India*
[5]*Department of Physics, Baylor University, One Bear Place 97316, Waco, TX76798-7316, USA*
[6]*Department of Physics, University of South Florida, Tampa, FL 33620, USA*
(Dated: December 24, 2022)

The metal-to-insulator phase transition (MIT) in low-dimensional materials and particularly two-dimensional layered semiconductors is exciting to explore due to the fact that it challenges the prediction of Abrahams *et al.* [1] that a two-dimensional system must be insulating at low temperatures. Thus, the exploration of MITs in 2D layered semiconductors expands the understanding of the underlying physics. Here we report the MIT of a few-layered $MoSe_2$ field effect transistor under a gate bias (electric field) applied perpendicular to the $MoSe_2$ layers. With low applied gate voltage, the conductivity as a function of temperature from 150 K to 4 K shows typical semiconducting to insulating character. Above a critical applied gate voltage, V_c, the conductivity becomes metallic (*i.e.*, the conductivity increases continuously as a function of decreasing temperature). Evidence of a metallic state was observed using an applied gate voltage or, equivalently, increasing the density of charge carriers within the 2D channel. We analyzed the nature of the phase transition using percolation theory, where conductivity scales with the density of charge carriers as $\sigma \propto (n\text{-}n_c)^{\delta}$. The critical exponent for a percolative phase transition, δ(T), has values ranging from 1.34 (at T = 150 K) to 2 (T = 20 K), which is close to the theoretical value of 1.33 for percolation to occur. Thus we conclude that the MIT in few-layered $MoSe_2$ is driven by charge carrier percolation. Furthermore, the conductivity does not scale with temperature, which is a hallmark of a quantum critical phase transition.

Keywords: Field-effect transistor, phase transition, conductivity, percolation, critical exponent.

I. INTRODUCTION

The emergence of complex states of matter near zero temperature phase transitions has produced fascinating quantum phenomena that need to be investigated in different materials with varying characteristics, such as bandgap size, number of layers, and applied external sources of electric, magnetic fields or pressure. Future electronic technologies will likely rely on materials where these emergent, cooperative behaviors can be tuned and manipulated. In particular, phase transitions in quantum materials, especially low-dimensional 2D semiconductors, are significantly affected by the quality of the materials (defects, disorder and impurities) as well as the number of layers [2]. Close to a phase transition, the interplay between these different types of fluctuations can cause many unconventional phenomena that can change the critical point and nature of an MIT. These intrinsic and extrinsic parameters substantially change the nature of the phase transition in ways that are not currently understood. Defects and disorder play a significant role in the observed 2D charge state, whose properties are often further complicated by strong electron correlations. As a result, 2D conductivity has exhibited a metal-insulator transition (MIT) governed either by metallic regions percolating through the background insulating state or by quantum fluctuations near a potential quantum critical point.

Perhaps the oldest, but also among the least understood, example of correlated electron phenomena is the metal-to-insulator phase transition. Developing a better understanding of the MIT is an important research goal, and identifying semiconducting materials that change from insulating to metallic at low temperatures has a wide range of potential applications such as in quantum computation. Materials in which an MIT can be induced have vastly different physical properties controlled by external manipulation of parameters like charge-carrier concentration, pressure, temperature, and magnetic field to name a few. This is in contrast, of course, to simple elemental metals and insulators whose properties are essentially constant.

The MI transition is a significant problem within materials physics not only because of the technological promise a better understanding of it holds, but also because it is one of the best examples of quantum-critical physics [3]. The hallmark of quantum-critical physics is the identification of a quantum-critical point, where a continuous phase transition occurs at zero temperature in the phase

* Corresponding Email: nihar.r.pradhan@jsums.edu
Email: mcgill@magnet.fsu.edu

diagram. Since a qualitative distinction between a conductor and an insulator really exists only at zero temperature ($T = 0$ K) (*i.e.*, the conductivity σ ($T = 0$ K) $\neq 0$ in the metal, and σ ($T = 0$ K) $= 0$ in the insulator), it is the quantum fluctuations of the charge carriers at zero temperature that govern the critical distinctions. In such a way, it is expected that studying the MIT in the layered 2D semiconductors should provide an excellent window for investigating physics near a quantum-critical point.

A few research groups recently reported various aspects of MITs in 2D systems. An MIT in MoS_2 was reported by Radisavljevic and Kis [4], suggesting the origin of the phase transition was strong electron-electron interactions under high carrier doping permitted by the top HfO_2 gate dielectric. An increase in conductivity with decreasing temperature suggested the occurrence of an MIT. The intrinsic mechanism and type of interaction of charge carriers are still elusive due to the various levels of carrier-carrier interactions in 2D systems. Pradhan *et al.*, [5] carried out a similar study on few-layered ReS_2 fabricated on a Si/SiO_2 substrate without any dielectric engineering. The four-terminal conductivity data strongly suggested that the increase in conductivity as a function of temperature occurred above a certain applied gate voltage at which the density of charge carriers could drive the MIT in ReS_2 by strong electron-electron interactions. The resistivity of ReS_2 further showed a Fermi-liquid-like behavior, and the temperature-scaling showed evidence of a quantum phase transition. Moon *et al.*, [6, 7] reported a similar quantum phase transition with temperature scaling. Another similar temperature-dependent scaling also gave support for a quantum phase transition in WSe_2 encapsulated with h-BN [8]. These reports suggested the quantum-critical nature of the phase transitions in the 2D semiconductors with different levels of doping. On the other hand, a percolative phase transition was reported in the ternary compound $CuIn_7Se_{11}$, where the temperature-dependent conductivity fit well with percolation theory [9].

Here, we explored the intrinsic nature of the MIT in few-layered $MoSe_2$ fabricated on a Si/SiO_2 substrate without high-k dielectric engineering. Further details regarding the $MoSe_2$ crystals and the fabrication method are given in the methods section. The nature of the phase transition is studied using multi-terminal transport measurements carried out at different temperatures and through interpretations of the experimental data using theoretical temperature scaling analysis.

II. RESULTS AND DISCUSSION

Figure 1 (a) shows an optical image of the device and the transport measurement layout with four contacts fabricated on the Si/SiO_2 substrate. The contacts were fabricated using standard optical lithographic techniques, followed by the e-beam evaporation of Au(80nm)/Cr(5nm) at a base pressure of 10^{-8} Torr. The thickness of the $MoSe_2$ layer was 7 nm as measured by atomic force microscopy. The device was covered with a thin layer of Cytop polymer to maintain its pristine nature without exposing it to air/oxygen. Cytop does not dope or change any electronic characteristic of the device based on our previous reports, it rather forms a barrier to moisture and oxygen exposure from the atmosphere [5, 10, 11]. Highly p-doped Si was used for the back gate to control the charge carrier density inside the channel.

Figure 1 (b) shows the drain-source current (I_{ds}) as a function of drain-source voltage (V_{ds}) measured using standard four-terminal geometry at room temperature. The I-V curve exhibited a non-linear dependence between 0 and 300 mV at all applied gate voltages due to Schottky barrier formation at the semiconductor-metal junctions. 2D semiconducting materials composed of single to few-atomic layers are prone to form Schottky contacts due to Fermi level pinning (FLP) at the interface, which arises from the difference in the work function between the metal and semiconductor [12]. The work function of few-layered $MoSe_2$ is ~ 4.6 eV and for Cr is 4.5 eV [13, 14]. The Schottky barrier height is the difference between electron affinity of $MoSe_2$ and the work function of the metal contact Cr deposited on the $MoSe_2$. Theoretically the electron affinity of few-layered $MoSe_2$ is $\sim$4.0 eV. One would expect the Schottky barrier height is $\sim$300 meV. The experimentally measured Schottky barrier may be different than theoretical prediction due to factors such as disorder-induced carrier localization and contact resistance, if measured in a 2-terminal geometry that can influence the behavior of the conduction mechanism across the contacts [10, 15]. Theoretically, a Schottky barrier height of ~ 300 meV could be present. This barrier height may vary with the number of semiconducting layers [12]. For monolayer $MoSe_2$ with contacts of 3D metals, strong pinning is found at the metal-semiconductor (M–S) interface [16–18]. The FLP originates from several factors, such as the formation of an electric dipole at the interface due to a change of the charge distribution at the junction and metal, and defect/disorder-induced gap states [18–20]. The pinning may be less pronounced in multi-layered $MoSe_2$ compared to a monolayer. The charge accumulation in multilayers is larger than that in a monolayer, which might reduce the pinning effect.

Figure 1 (c) shows I_{ds} versus V_{bg} measured at 200 K as a reference for Figure 1 (d) which shows the same data recorded at 5.7 K. At 200 K, the threshold for the ON state has increased significantly from that at room temperature, where thermionic emission can play a greater role in promoting charge carriers into the conduction band. At the lowest temperatures, the remaining charge density in the conduction band is mostly due to intrinsic doping occurring during crystal growth. Our data demonstrate that the $MoSe_2$ device showed high electron doping, as previously reported by several research groups [21–24]. The electron-doped behavior in $MoSe_2$

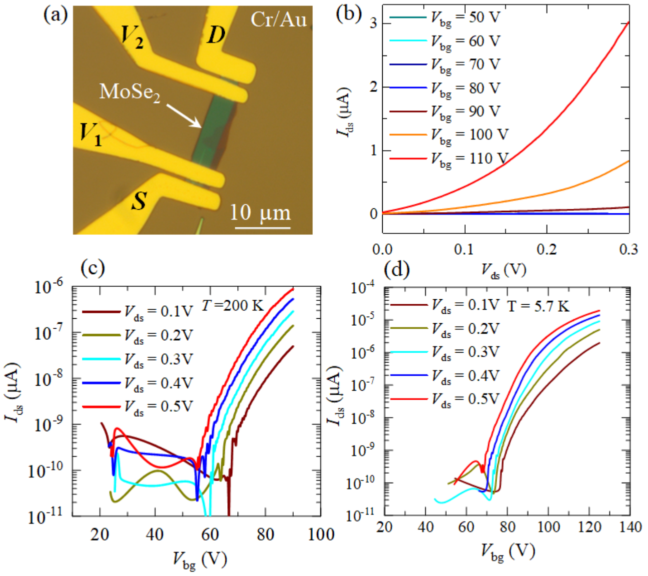

FIG. 1. (a) Optical micrograph image of one of the MoSe$_2$ FET device fabricated on the Si/SiO$_2$ wafer. The thickness of the MoSe$_2$ is 7 nm (∼10 layers) measured using AFM. (b) Drain-source current as a function of drain-source voltage at several applied V_{bg}. (c) Drain-source current in semi-logarithmic scale as a function of V_{bg} at V_{ds}=0.1 - 0.5 V measured at 200 K. (d) Same I_{ds} vs V_{bg} graph but measured at T =5.7 K.

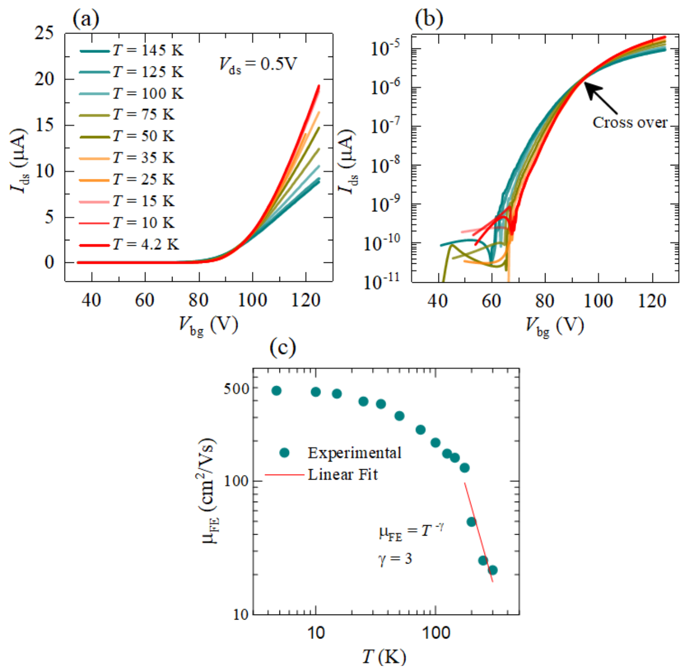

FIG. 2. (a) Linear plot of I_{ds} as a function of V_{bg} measured at several different temperatures and constant V_{ds} =0.5V. (b) Semi-logarithmic plot of the same I_{ds} shows cross-over temperature, while cooling indicates the transition at certain applied V_{bg}. (c) Temperature-dependent field-effect carrier mobility as a function of T. The red line shows the linear fit to the mobility values using the depicted equation within the Figure.

is found to originate from the high density of Se vacancies in MoSe$_2$, similar to the S-vacancy in MoS$_2$ crystals [25, 26]. It is clear that at 5.7 K, higher V_{bg} is required to turn the device ON, but it is also apparent that the slope of the current rise in the ON state has increased. As the temperature decreases, less thermal energy is available to free charges trapped by defects and disorder. Therefore, if we study the temperature dependence of the field-effect charge mobility, we can learn about the processes that control charge localization in the MoSe$_2$ devices.

Figure 2 displays the temperature-dependent field effect transport of the MoSe$_2$ FET. I_{ds} as a function of V_{bg} at fixed V_{ds} = 500 mV is shown in Fig. 2 (a). The FET showed the minimum current at applied V_{bg} up to 50 V which indicateed the OFF state of the transistor. When the gate voltage was swept higher, the current increased exponentially, confirming the ON state of the transistor. As shown in Fig. 2 (b), a semilog plot of the same data demonstrated that there was a temperature below which I_{ds} crossed over to higher values than it achieved at more elevated temperatures. The current ratio of the FET between the ON and OFF states was 10^5, which was similar to that reported for other multilayer MoSe$_2$ FETs [27–29]. In Fig. 2 (c), we plotted the field-effect mobility versus temperature. We used $\mu_{FE} = \frac{l}{W} \times \frac{1}{C_i} \times \frac{d(I_{ds}-I_o)}{dV_{bg}}$, where W = 6 μm was the width and C_i was the capacitance per unit area of the device. For 285 nm thick SiO$_2$, we calculated C_i = 12.738 × 10^{-9} F. l = 12 μm was the channel length between the two voltage leads V_1 and V_2. The average mobility of the few-layered MoSe$_2$ FETs displayed maximum room temperature field-effect mobilites between 20 and 35 cm^2/Vs while showing a remarkable increase with decreasing temperature to nearly 500 cm^2/Vs at 4 K. The sharp increase in mobility was observed mainly between room temperature and 100 K due to the suppression of phonon scattering [30–33]. The saturation of mobility below 100 K suggested that impurity scattering, carrier localization, or suppression of thermionic emission of carriers across the Schottky barriers limited charge transport at low temperatures [5, 34, 35]. The exponent γ obtained from fitting mobility as a function of temperature in Fig. 2(c) reflected the phonon scattering process in MoSe$_2$, and the value was about 3, which is comparable to previously reported values for 2D materials [5, 9, 36]. The higher the value of the exponent, the stronger phonon scattering suppression occurs with decreasing temperature. The soft optical phonons are major scattering agents at high temperature. The sharp rise in mobility is associated with the soft optical phonon scattering suppression as previously reported [37].

We decided to perform a deeper analysis of the temperature-dependent conductivity of the MoSe$_2$ devices. By comparing the conductivities of the devices to theories of electron-transport, a better understand-

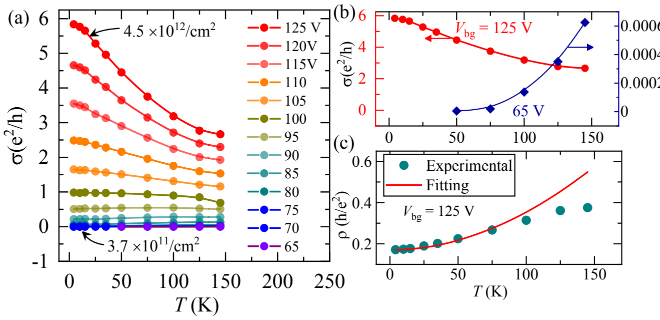

FIG. 3. (a) Conductivity (in multiples of the quantum conductance) vs temperature at several applied gate voltages extracted from the FET transport measurements. (b) Conductivity vs temperature at V_{bg} = 65 V and 125 V. (c) shows the resistivity versus temperature at the applied gate voltage V_{bg}=125 V. The line is a Fermi-Liquid fit to the low-temperature, metallic portion of the data.

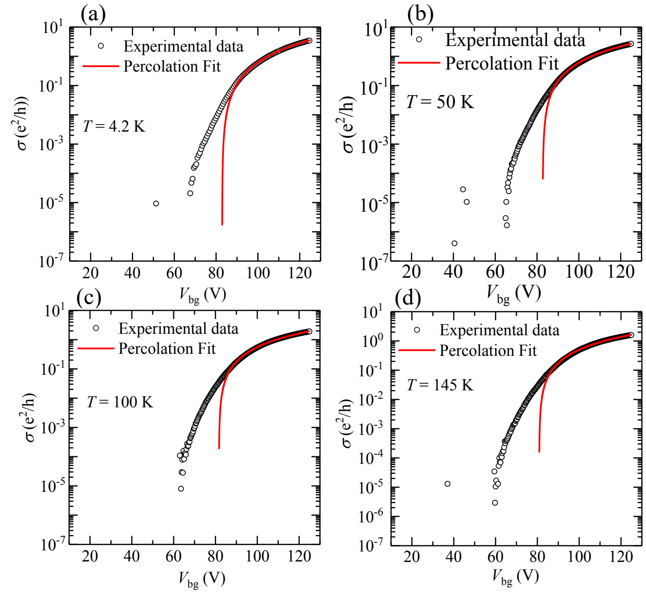

FIG. 4. Conductivity vs V_{bg}: Experimental data and fitting using temperature scaling percolation theory through the equation $\sigma = (n\text{-}n_c)^{\delta} \propto (V\text{-}V_o)^{\delta}$ (see text) for temperatures (a) 4.2K, (b) 50K, (c) 100K and (d) 145K.

ing of the fundamental processes involved in the electron transport of few-layered $MoSe_2$ channels can be attained. Figure 3(a) displays the conductivity versus temperature for several different gating voltages (75 V to 125 V) or, equivalently, induced carrier densities. The carrier density ranged from $n = 3.7 \times 10^{11}/\mathrm{cm}^2$ to $4.5 \times 10^{12}/\mathrm{cm}^2$ as obtained from the relation $ne = C_i\ |(V_{bg}\text{-}V_{th})|$. Below the applied gate voltage $V_{bg} < 90$V, σ decreased with decreasing temperature and for $V_{bg} > 90$V, σ increased with decreasing T as displayed in Fig. 3 (a). The two conductivity plots in Fig. 3(b) indicated that $MoSe_2$ was a typical semiconductor at V_{bg} = 65 V. Surprisingly, at V_{bg} = 125 V (i.e., high carrier density), σ increased monotonically as T decreased, indicating metallic conductivity. This data demonstrated that a clear metallic phase emerged at high carrier density from the insulating behavior at low electron concentrations. At low-carrier concentration conductivity decreased with decreasing temperature following a typical semiconducting trend but when the carrier concentration increased (V_{bg} = 125 V), as shown in Figure 1(b), the conductivity also increased throughout the temperature range displayed. This insulating to metallic branch of conductivity was evident from the semi-logarithmic plot of the conductivity as a function of temperature presented in the supporting information (see Supporting information Fig. 1). The resistivity $\rho = (\sigma)^{-1}$ of the sample as a function of T displayed in Figure 3(b) indicated metallic behavior as it matched the typical metallic Fermi-liquid like T-dependence ($\rho_o + AT^2$) up to almost 100 K which is also where the current crossover was observed (see Fig. 2 (b)), where ρ_o is the residual resistivity. To elucidate the nature of the phase transition, we used scaling analysis, which is one of the well-established theoretical methods to check the nature of a phase transition. This analysis indicated that the observed phase transition could be described as a percolation-type transition at higher temperatures.

We analyzed the conductivity data through temperature scaling percolation theory, shown in Figs. 4(a-d), which describes the conditions under which the charge clusters appearing at the interface of the gate dielectric and 2D semiconductor can form an interconnected random network [9, 38]. The conductivity scaling follows $\sigma\ (T{=}0) = (n\text{-}n_c)^{\delta}$, where conductivity percolation exponent, δ, has a value for a 2D MIT of $\sim 4/3$ denoting the point at which the random network becomes interconnected [9, 38–40]. Since the density of the charge carriers varies proportionally with the applied gate voltage and assuming $n = C_{ox}\ (V_{bg}\text{-}V_{th})$, where V_{th} is the threshold gate voltage, we can fit the conductivity as a function of gate voltage as $\sigma = (n\text{-}n_c)^{\delta} \propto (V_{bg}\text{-}V_o)^{\delta}$. The parameters n and n_c are the carrier density and the critical carrier density, respectively, below which the T-dependent conductivity is insulating while exhibiting a metallic behavior above it. V_o is the critical back gate voltage that needs to be extracted from the fitting. The value of n_c is calculated from σ_c identified from the σ vs T graph (Fig. 3) which showed almost no temperature dependence.

Fitting of σ in different temperature regions is shown in Fig. 4. A better fit to the conductivity data was seen in the high gate voltage (*i.e.*, high carrier density) range compared to the low gate voltage range (*i.e.*, low carrier density), similar to the percolation fitting predicted in the earlier reports of MITs in Si-MOSETs, MoS_2 and $CuIn_7Se_{11}$ [9, 38, 41]. The extracted values of the T-dependent exponent δ are plotted in Fig. 5 (upper panel) as a function of temperature. The value of $\delta = 1.34$ was a close match with the known theoretical percolation MIT value for a 2D system from 80 K to 150 K. The decrease of exponent δ with an increase in temperature indicated

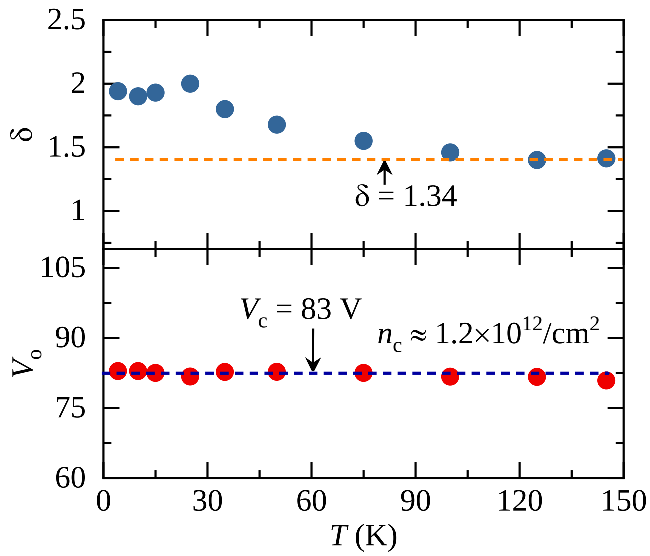

FIG. 5. (Upper Panel) Exponent δ obtained from the percolation fitting is plotted as a function of T. (Lower Panel) Extracted V_c value from the fitting from where critical charge carrier density n_c was extracted.

a phonon contribution. The deviation of δ below 80 K could have been due to the non- critical temperature dependent contribution realizing that at any finite temperature the material behaves like an effective metal as the conductivity does not vanish. Impurity scattering may also have played a significant role in the deviation of δ above 1.34.

This scaling of the MIT in few-layer $MoSe_2$ was very similar to the reported percolation MITs in low-disorder Si-MOSFETs [38]. A similar percolation type of MIT and a critical exponent were also reported in 2D layered ternary material, $CuIn_7Se_{11}$ [9]. The fitted values of the critical voltage $V_c = V_o$ are shown in Fig. 4 (lower panel) as a function of temperature. The average value of $V_c = 83$ V, and the extracted critical density of the charge carriers corresponding to V_c was $n_c = 1.2{\times}10^{12}$ cm^{-2}. A critical carrier density that was two orders of magnitude lower has been reported in 2D $CuIn_7Se_{11}$ and Si-MOSFET. The critical exponent consistent with the 2D percolation phase transition suggested that the MIT was governed by percolation. The critical carrier density calculated here was from the value V_o, obtained from the fitting of the conductivity data with the percolation relation. This extracted value was lower than the crossover gate voltage $V_{bg} \approx 92$ V shown in Figs. 2(a-b).

As reported earlier, the MIT phenomenon in other materials such as MoS_2, ReS_2 and WSe_2 [5, 7, 8] showed quantum critical behavior. We also checked by fitting our temperature-dependent conductivity σ (n,T) data to quantum critical scaling [5, 42–44]. The detailed temperature scaling is given in the supporting information and Figures S1 and S2. The conductivity can be expressed as $\sigma\ (n,T) \sim F\ (T/T_o)$, where F is the universal scaling function, $T_o = T_o\ (n) \sim |n\text{-}n_o|^\gamma$, where the exponent $\gamma = z\nu$ is a product of the correlation exponent, ν, and the dynamical exponent, z. To reveal the quantum criticality, the T-dependent conductivity of $MoSe_2$ should scale as a function of the temperature parameter T/T_o, where T_o is the temperature scaling parameter. In this scaling, all the metallic and insulating conductivity branches should collapse to a single curve. As shown in Fig. S2 of the supplementary information, the normalized conductivity data with critical conductivity, σ/σ_c, reflected the separation of the metallic conductivity from the insulating branch. The critical conductivity, σ_c, was chosen from the T-dependent conductivity curves, which took the power law form $\sigma_c\ (T \to 0) \propto T^x$ or, on a logarithmic scale, $\sigma\ (T,n)$ does not vary as a function of temperature. To indicate quantum critical behavior, all the metallic and insulating branches of the conductivity should collapse to a single curve with an appropriately chosen temperature parameter, T_o. Yet, we have not been able to obtain any similar scaling collapse of the conductivity data for the above $MoSe_2$ sample as shown in the supporting information Figure S2 (right panel), which indicated the absence of a quantum phase transition (QPT).

III. CONCLUSION

We fabricated high mobility field effect transistors using few-layer $MoSe_2$. Four-terminal measurements of I_{ds} versus V_{ds} and I_{ds} versus V_{bg} were collected over a temperature range from room temperature to 5 K. The conductivity of the few-layer $MoSe_2$ was calculated, and its temperature-dependence was plotted. Conductivity versus temperature demonstrated that an insulator-metal transition occurred in $MoSe_2$ at a specific critical charge-carrier density induced by the applied back gate voltage. Furthermore, the insulator-metal transition was consistent with the percolation of metallic clusters in a background insulating matrix according to expectations based on a scaling analysis of the calculated conductivity using percolation theory. We did not observe evidence for a quantum phase transition in $MoSe_2$, as has been recently observed for other similar 2D systems. The observation of MITs in various 2D monolayer and few-layered materials challenges long-held ideas about the fundamental nature of electron transport in two dimensions. As a result, the study of this phenomenon is imperative for fundamental science and could lead to the engineering of devices with novel properties for electronics and optoelectronics.

IV. MATERIALS AND METHODS

High quality $MoSe_2$ crystals grown using the flux method were purchased from 2DSemiconductor, USA.

Few-layered $MoSe_2$ flakes were mechanically exfoliated using the scotch tape technique and then transferred onto a clean Si substrate with a 285 nm thick SiO_2 layer. We verified the crystals with Raman spectroscopy measurements and it matched with the Raman spectra of 2H-$MoSe_2$ crystals in many reports, as well as the Raman spectra of the crystals provided by 2DSemiconductor. Atomic force microscopy was used to measure the thickness of the exfoliated flakes. All the processes were carried out inside the clean room environment at the Center for Nanoscale Materials, Argonne National Laboratory. Metal contacts were fabricated using a Direct Laser Pattern Generator (Microtech LW405) and followed thereafter by the e-beam evaporation of Au(80nm)/Cr(5 nm) (Lesker PVD 250) at pressures of 10^{-8} Torr, lift-off, and vacuum annealing. The devices were encapsulated with a 20 nm thick Cytop layer (amorphous fluoropolymer). Keithley instruments 2612B and 2635 source meters were used to perform electrical measurements in vacuum. All the temperature-dependent measurements were performed using a temperature-controlled cryogenic cell with liquid Helium cooling system. Transport measurement were performed using a four-terminal configurations.

ACKNOWLEDGMENTS

Use of the Center for Nanoscale Materials, a Department of Energy Office of Science User Facility, was supported by the U.S. DOE, Office of Basic Energy Sciences, under Contract No. DE-AC02-06CH11357. N. R. P. acknowledged NSF-PREM through NSF-DMR-1826886, HBCU-UP Excellence in research NSF-DMR-1900692. A portion of this work was performed at the National High Magnetic Field Laboratory, which is supported by the National Science Foundation Cooperative Agreement No. DMR-1644779 and the State of Florida.

Supporting Information: The supplementary materials contain the semi-logarithmic graph of the conductivity to visualize clearly the insulating and metallic phase and temperature scaling of the conductivity to check the quantum critical nature of the phase transition.

[1] E. Abrahams, P. Anderson, D. Licciardello, and T. Ramakrishnan, Scaling theory of localization: Absence of quantum diffusion in two dimensions, Physical Review Letters **42**, 673 (1979).

[2] W. Zhou, S. Zhang, S. Guo, Y. Wang, J. Lu, X. Ming, Z. Li, H. Qu, and H. Zeng, Designing sub-10-nm metal-oxide-semiconductor field-effect transistors via ballistic transport and disparate effective mass: The case of two-dimensional bi n, Physical Review Applied **13**, 044066 (2020).

[3] T. Li, S. Jiang, L. Li, Y. Zhang, K. Kang, J. Zhu, K. Watanabe, T. Taniguchi, D. Chowdhury, L. Fu, *et al.*, Continuous mott transition in semiconductor moiré superlattices, Nature **597**, 350 (2021).

[4] B. Radisavljevic and A. Kis, Mobility engineering and a metal–insulator transition in monolayer mos2, Nature materials **12**, 815 (2013).

[5] N. R. Pradhan, A. McCreary, D. Rhodes, Z. Lu, S. Feng, E. Manousakis, D. Smirnov, R. Namburu, M. Dubey, A. R. Hight Walker, *et al.*, Metal to insulator quantum-phase transition in few-layered res2, Nano letters **15**, 8377 (2015).

[6] B. H. Moon, J. J. Bae, M.-K. Joo, H. Choi, G. H. Han, H. Lim, and Y. H. Lee, Soft coulomb gap and asymmetric scaling towards metal-insulator quantum criticality in multilayer mos2, Nature communications **9**, 1 (2018).

[7] B. H. Moon, G. H. Han, M. M. Radonjić, H. Ji, and V. Dobrosavljević, Quantum critical scaling for finite-temperature mott-like metal-insulator crossover in few-layered mos 2, Physical Review B **102**, 245424 (2020).

[8] L. J. Stanley, H.-J. Chuang, Z. Zhou, M. R. Koehler, J. Yan, D. G. Mandrus, and D. Popovic, Low-temperature 2d/2d ohmic contacts in wse2 field-effect transistors as a platform for the 2d metal–insulator transition, ACS Applied Materials & Interfaces **13**, 10594 (2021).

[9] P. D. Patil, S. Ghosh, M. Wasala, S. Lei, R. Vajtai, P. M. Ajayan, A. Ghosh, and S. Talapatra, Gate-induced metal–insulator transition in 2d van der waals layers of copper indium selenide based field-effect transistors, ACS nano **13**, 13413 (2019).

[10] N. Pradhan, D. Rhodes, S. Memaran, J. Poumirol, D. Smirnov, S. Talapatra, S. Feng, N. Perea-Lopez, A. Elias, M. Terrones, *et al.*, Hall and field-effect mobilities in few layered p-wse 2 field-effect transistors, Scientific reports **5**, 8979 (2015).

[11] N. R. Pradhan, C. Garcia, J. Holleman, D. Rhodes, C. Parker, S. Talapatra, M. Terrones, L. Balicas, and S. A. McGill, Photoconductivity of few-layered p-wse2 phototransistors via multi-terminal measurements, 2D Materials **3**, 041004 (2016).

[12] Q. Wang, Y. Shao, P. Gong, and X. Shi, Metal-2d multilayered semiconductor junctions: layer-number dependent fermi-level pinning, Journal of Materials Chemistry C **8**, 3113 (2020).

[13] P. Panigrahi, T. Hussain, A. Karton, and R. Ahuja, Elemental substitution of two-dimensional transition metal dichalcogenides (mose2 and mote2): implications for enhanced gas sensing, ACS sensors **4**, 2646 (2019).

[14] S. Choi, Z. Shaolin, and W. Yang, Layer-number-dependent work function of mos2 nanoflakes, Journal of the Korean Physical Society **64**, 1550 (2014).

[15] N. R. Pradhan, D. Rhodes, S. Feng, Y. Xin, S. Memaran, B.-H. Moon, H. Terrones, M. Terrones, and L. Balicas, Field-effect transistors based on few-layered α-mote2, ACS nano **8**, 5911 (2014).

[16] K. Sotthewes, R. Van Bremen, E. Dollekamp, T. Boulogne, K. Nowakowski, D. Kas, H. J. Zand-

vliet, and P. Bampoulis, Universal fermi-level pinning in transition-metal dichalcogenides, The Journal of Physical Chemistry C **123**, 5411 (2019).
[17] C. Kim, I. Moon, D. Lee, M. S. Choi, F. Ahmed, S. Nam, Y. Cho, H.-J. Shin, S. Park, and W. J. Yoo, Fermi level pinning at electrical metal contacts of monolayer molybdenum dichalcogenides, ACS nano **11**, 1588 (2017).
[18] D. S. Schulman, A. J. Arnold, and S. Das, Contact engineering for 2d materials and devices, Chemical Society Reviews **47**, 3037 (2018).
[19] M. Farmanbar and G. Brocks, First-principles study of van der waals interactions and lattice mismatch at mos 2/metal interfaces, Physical Review B **93**, 085304 (2016).
[20] J. Kang, W. Liu, D. Sarkar, D. Jena, and K. Banerjee, Computational study of metal contacts to monolayer transition-metal dichalcogenide semiconductors, Physical Review X **4**, 031005 (2014).
[21] D. Somvanshi, E. Ber, C. S. Bailey, E. Pop, and E. Yalon, Improved current density and contact resistance in bilayer mose2 field effect transistors by alo x capping, ACS applied materials & interfaces **12**, 36355 (2020).
[22] S. Hong, H. Im, Y. K. Hong, N. Liu, S. Kim, and J. H. Park, n-type doping effect of cvd-grown multilayer mose2 thin film transistors by two-step functionalization, Advanced Electronic Materials **4**, 1800308 (2018).
[23] Y. Jeong, H. J. Lee, J. Park, S. Lee, H.-J. Jin, S. Park, H. Cho, S. Hong, T. Kim, K. Kim, *et al.*, Engineering mose2/mos2 heterojunction traps in 2d transistors for multilevel memory, multiscale display, and synaptic functions, npj 2D Materials and Applications **6**, 1 (2022).
[24] A. Rani, S. Guo, S. Krylyuk, K. DiCamillo, R. Debnath, A. V. Davydov, and M. E. Zaghloul, Electronic characteristics of mose 2 and mote 2 for nanoelectronic applications, in *2018 IEEE 13th Nanotechnology Materials and Devices Conference (NMDC)* (IEEE, 2018) pp. 1–4.
[25] J. Yang, H. Kawai, C. P. Y. Wong, and K. E. J. Goh, Electrical doping effect of vacancies on monolayer mos2, The Journal of Physical Chemistry C **123**, 2933 (2019).
[26] E. Mitterreiter, B. Schuler, A. Micevic, D. Hernangómez-Pérez, K. Barthelmi, K. A. Cochrane, J. Kiemle, F. Sigger, J. Klein, E. Wong, *et al.*, The role of chalcogen vacancies for atomic defect emission in mos2, Nature communications **12**, 1 (2021).
[27] W. Wu, D. De, S.-C. Chang, Y. Wang, H. Peng, J. Bao, and S.-S. Pei, High mobility and high on/off ratio field-effect transistors based on chemical vapor deposited single-crystal mos2 grains, Applied Physics Letters **102**, 142106 (2013).
[28] N. R. Pradhan, D. Rhodes, Y. Xin, S. Memaran, L. Bhaskaran, M. Siddiq, S. Hill, P. M. Ajayan, and L. Balicas, Ambipolar molybdenum diselenide field-effect transistors: field-effect and hall mobilities, Acs Nano **8**, 7923 (2014).
[29] N. R. Pradhan, Z. Lu, D. Rhodes, D. Smirnov, E. Manousakis, and L. Balicas, An optoelectronic switch based on intrinsic dual schottky diodes in ambipolar mose2 field-effect transistors, Advanced Electronic Materials **1**, 1500215 (2015).
[30] M. Madusanka Perera, M.-W. Lin, H.-J. Chuang, B. Prasad Chamlagain, C. Wang, X. Tan, M. Ming-Cheng Cheng, D. Tománek, and Z. Zhou, Improved carrier mobility in few-layer mos2 field-effect transistors with ionic-liquid gating, arXiv e-prints , arXiv (2013).
[31] J. Jiang, Y. Zhang, A. Wang, J. Duan, H. Ji, J. Pang, Y. Sang, X. Feng, H. Liu, and L. Han, Construction of high field-effect mobility multilayer mos2 field-effect transistors with excellent stability through interface engineering, ACS Applied Electronic Materials **2**, 2132 (2020).
[32] H. K. Ng, D. Xiang, A. Suwardi, G. Hu, K. Yang, Y. Zhao, T. Liu, Z. Cao, H. Liu, S. Li, *et al.*, Improving carrier mobility in two-dimensional semiconductors with rippled materials, Nature Electronics , 1 (2022).
[33] L. Cheng, C. Zhang, and Y. Liu, Intrinsic charge carrier mobility of 2d semiconductors, Computational Materials Science **194**, 110468 (2021).
[34] N. R. Pradhan, C. Garcia, M. C. Lucking, S. Pakhira, J. Martinez, D. Rosenmann, R. Divan, A. V. Sumant, H. Terrones, J. L. Mendoza-Cortes, *et al.*, Raman and electrical transport properties of few-layered arsenic-doped black phosphorus, Nanoscale **11**, 18449 (2019).
[35] H. C. Movva, A. Rai, S. Kang, K. Kim, B. Fallahazad, T. Taniguchi, K. Watanabe, E. Tutuc, and S. K. Banerjee, High-mobility holes in dual-gated wse2 field-effect transistors, ACS nano **9**, 10402 (2015).
[36] N. R. Pradhan, J. Ludwig, Z. Lu, D. Rhodes, M. M. Bishop, K. Thirunavukkuarasu, S. A. McGill, D. Smirnov, and L. Balicas, High photoresponsivity and short photoresponse times in few-layered wse2 transistors, ACS applied materials & interfaces **7**, 12080 (2015).
[37] N. Ma and D. Jena, Charge scattering and mobility in atomically thin semiconductors, Physical Review X **4**, 011043 (2014).
[38] S. D. Sarma, M. Lilly, E. Hwang, L. Pfeiffer, K. West, and J. Reno, Two-dimensional metal-insulator transition as a percolation transition in a high-mobility electron system, Physical review letters **94**, 136401 (2005).
[39] L. Tracy, E. Hwang, K. Eng, G. Ten Eyck, E. Nordberg, K. Childs, M. Carroll, M. Lilly, and S. D. Sarma, Observation of percolation-induced two-dimensional metal-insulator transition in a si mosfet, Physical Review B **79**, 235307 (2009).
[40] S. He and X. Xie, New liquid phase and metal-insulator transition in si mosfet s, Physical review letters **80**, 3324 (1998).
[41] B. H. Moon, J. J. Bae, G. H. Han, H. Kim, H. Choi, and Y. H. Lee, Anomalous conductance near percolative metal–insulator transition in monolayer mos2 at low voltage regime, ACS nano **13**, 6631 (2019).
[42] S. Kravchenko, W. E. Mason, G. Bowker, J. Furneaux, V. Pudalov, and M. D'iorio, Scaling of an anomalous metal-insulator transition in a two-dimensional system in silicon at b= 0, Physical Review B **51**, 7038 (1995).
[43] E. Abrahams, S. V. Kravchenko, and M. P. Sarachik, Metallic behavior and related phenomena in two dimensions, Reviews of modern physics **73**, 251 (2001).
[44] V. Dobrosavljevic, N. Trivedi, and J. M. Valles Jr, *Conductor insulator quantum phase transitions* (Oxford University Press, 2012).